East European Journal of Physics. **2.** 247-251 (2025)
DOI:10.26565/2312-4334-2025-2-29 ISSN 2312-4334

TEMPERATURE AND INFRARED QUENCHING OF EQUILIBRIUM CONDUCTIVITY IN $CdSe_xS_{1-x}$ FILM

Valijon T. Mirzaev, Bozorboy J. Akhmadaliyev, Iftikhorjon I. Yulchiev, Muminjon M. Madraximov, Tokhirbek I. Rakhmonov*
Fergana State Technical University, Fergana, Uzbekistan
**Corresponding Author e-mail: radiofizik2014@gmail.com*
Received January 29, revised March 17, 2025; accepted April 8,2025

A method for obtaining *CdSe, $CdSe_xS_{1-x}$* films with high photosensitivity has been developed. This method involves thermal treatment of freshly prepared films in vacuum and air in a specially prepared quasi-hermetic chamber in the presence of *$CdCl_2$* or *$CuCl_2$*, which ensures uniform diffusion of sensitizing substances. Experiments have shown that *CdSe, $CdSe_xS_{1-x}$* films with stable and reproducible electrophysical properties are obtained by heating at the following temperatures: in air in the presence of *$CdCl_2$* – 470°C*;* in the presence of *$CuCl_2$* – 300°C; in vacuum – 480°C. Temperature and infrared quenching of equilibrium conductivity are observed only in optimally photosensitive samples with both fast (r) and slow (s) recombination centers and efficiently operating intercrystalline barriers. However, various external influences significantly affect the carrier motion, leading to the loss of high photosensitivity of the sample. Infrared quenching of equilibrium conductivity is observed at $T < 300\ K$ and low infrared light intensities $I_{IR} < 10^{-1} lx$ in the entrance spectral absorption range of 1.0 ÷ 3.0μm, and a pronounced photoconductivity with a clearly defined entrance is observed at $I_{IR} \geq 10^{-1} lx$.
Keywords: *Photosensitivity; CdSe, $CdSe_xS_{1-x}$; Quasi-closed camera; Thermal treatment; Temperature and infrared quenching; Spatial charge field; Drift barriers; Grain size*
PACS: 72.20.My, 73.50.Gr, 77.55.-g, 78.55.Et, 81.15.-z

INTRODUCTION

The anomalous temperature dependence of the electrical conductivity of photosensitive CdSe, $CdSe_xS_{1-x}$ thin films with infrared quenching of the equilibrium conductivity was determined. The results of measurements and analysis of the kinetic parameters σ_d, n, μ in the dark for $CdSe_xS_{1-x}$:Cd:Cu:Cl samples with different thermal treatment methods in the range 300÷500 ^{0}C were carried out. It was found that the observed anomalous effects are associated with the excessive charge of bulk deep r-, s-centers in the spatial charge field and the modulation of this region and drift barriers at the grain boundaries upon heating or under the influence of infrared radiation. Previously, an anomalous temperature dependence of the electrical conductivity was found in a number of polycrystalline $CdSe_xS_{1-x}$ samples [1-2], which manifests itself in a sharp decrease in the dark current in a certain temperature range when the semiconductor is heated. In $CdSe_xS_{1-x}$:Cu:Cl films, the decrease in dark conductivity reached 7 orders of magnitude in the temperature range 200÷300 K [2-3]. Various authors attribute the occurrence of this effect to the unbalanced filling of trapping centers, the influence of humidity [1-5], intercrystal reactions [1], macroscopic barriers [2], diffusion processes and oxygen chemisorption [4], and thermo-field migration of ions [6]. There is still no single comprehensive opinion about the mechanism of this anomalous phenomenon. Our goal is to study the temperature dependence of the dark conductivity of photosensitive thin $CdSe_xS_{1-x}$ films, depending on the production technology and under the influence of weak infrared radiation.

TECHNOLOGY AND MEASUREMENT METHODS

To obtain $CdSe_xS_{1-x}$ films, we used the method of thermal evaporation in vacuum. A vacuum unit was assembled based on an automatically controlled vacuum unit VUP-5M and a "VAKMA" 2NVR-5 DM type fore vacuum pump, which provides a pressure of ~10^{-2} Pa and a "VAKMA" NVDM-160 vapor-oil diffusion pump (Figure 1). Polycrystalline $CdSe_xS_{1-x}$ films with dimensions of 5×25 mm^2 and a thickness of 5÷10 microns were obtained by evaporating a $CdSe_{0.8}S_{0.2}$ solid solution in a quasi-closed vacuum at a pressure of 10^{-2} Pa at a growth rate of 80÷100 Å/s, at an angle of 45^0, from a crucible heated to 300÷500 ^{0}C at a height of 9 cm above a glass substrate. The substrate and crucible temperatures were monitored using a "Chromel-Alumel" thermocouple on a PeakTech 3340 DMM thermometer [15-18]. The obtained films were subjected to thermal treatment in three ways: in a vacuum of 10^{-2} Pa at a temperature of 480 ^{0}C, in air in the presence of $CdCl_2$ at a temperature of 470 ^{0}C, and in the presence of $CuCl_2$ vapor at a temperature of 300 ^{0}C (Figure 2). The films obtained in this way (dark conductivity $\sigma_d \approx 10^{-5} \div 10^{-6}\ \Omega^{-1} \cdot m^{-1}$ at 300 K) were strongly compensated and had high photosensitivity $\sim 10^2$ lx under natural light intensity).

RESULTS OF THE EXPERIMENT AND THEIR DISCUSSIONS

We were able to observe a sharp decrease in the dark conductivity σ_d, the temperature quenching of the dark conductivity (TQDC), in high-resistance ($R_{film} > 10^9\ \Omega$) $CdSe_xS_{1-x}$ (Cd;Cu:Cl) films when the temperature was raised in the range of 150÷300 ^{0}C. Unlike the results presented in works [7-9], for the first time in these films, an inverse photoconductivity with an entrance character and infrared quenching of dark conductivity (IQDC) were identified. It was found that multiple heating-cooling cycles of films obtained in vacuum of 10^{-2} and 10^{-5} Torr and in air at T=77÷473 K in the dark for t=30 minutes do not affect the dependence of $\sigma_d\ (T)$ and the spectrum (IQDC) $\sigma_d\ (\lambda)$. Moreover, measurements of σ_d after a year did not reveal any significant changes in the $\sigma_d\ (T)$ and $\sigma_d\ (\lambda)$ spectra. The reproducibility of the observed effects is indicated by the balance of the re-measured σ_d value. Figure 3 shows the temperature dependence of the equilibrium conductivity for three samples: $CdSe_xS_{1-x}$ (curve 1) thermally treated in vacuum with a

Cite as: V.T. Mirzayev, B.J. Akhmadaliev, I.I. Yulchiev, M.M. Madraximov, T.I. Rakhmonov, East Eur. J. Phys. 2, 247 (2025), https://doi.org/10.26565/2312-4334-2025-2-29

residual gas pressure of 10^{-2} Pa, $CdSe_xS_{1-x}$ (CdCl) (2) and $CdSe_xS_{1-x}$ (CuCl) (3), treated in air in the presence of $CdCl_2$ and $CuCl_2$ vapor molecules, respectively.

It can be seen that all $\sigma_d\ (T)$ curves have two intervals of thermal quenching I and II. Within the measurement error, the "small" quenching (I) corresponds to the intervals 150÷230 K and the "large" quenching (II) to the intervals 230÷300 K for all samples. The activation energies determined from the slopes of curves 1-3 for section II are the same and equal to $E_r\ \approx 0.5$ eV, while for section I they differ slightly: 0.2 eV for CdSe (CdCl) and 0.3 eV for CdS (CdCl). However, it should be noted that these values do not accurately reflect the energy depth of the recombination centers responsible for the observed conductivity quenching [10-12]. In the temperature range T=400 K, a sharp increase in σ_d occurs with an activation energy of 1.5÷1.7 eV, which means that in this case, the dark conductivity is associated with the thermal generation of carriers characteristic of the intrinsic conductivity region of the semiconductor.

Figure 1. Schematic diagram of the vacuum chamber for obtaining $CdSe_xS_{1-x}$ films
1-crucible (evaporator); 2-shield; 3-furnace and substrate; 4-thermocouple; 6-metal cover

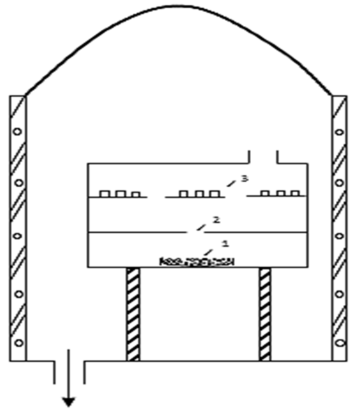

Figure 2. Schematic diagram of the chamber for increasing the sensitivity of $CdSe_xS_{1-x}$ films
1-crucibles; 2-slit for the entry of $CdCl_2$ or $CuCl_2$ vapors; 3-freshly prepared samples.

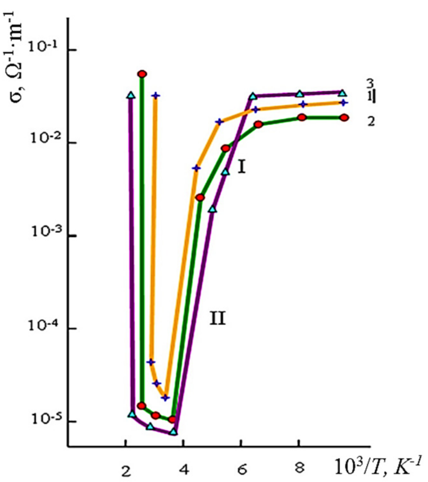

Figure 3. Temperature dependence of the equilibrium conductivity for three samples: $CdSe_xS_{1-x}$ (curve 1) thermally treated in vacuum with a residual gas pressure of 10^{-2} Pa, $CdSe_xS_{1-x}$ (CdCl) (2) and $CdSe_xS_{1-x}$ (CuCl) (3), treated in air in the presence of $CdCl_2$ and $CuCl_2$ vapor molecules, respectively.

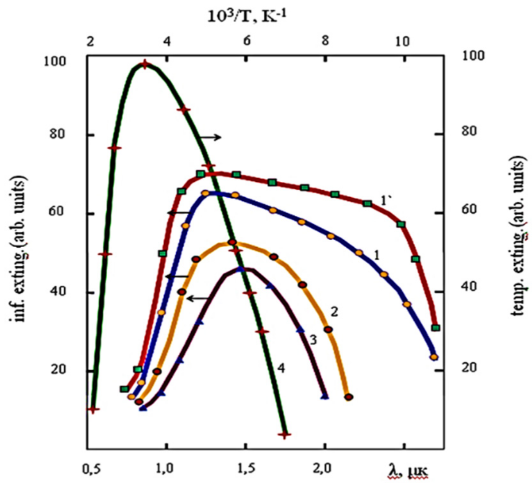

Figure 4. Infrared quenching spectra of the equilibrium conductivity Γ_{IR} of $CdSe_xS_{1-x}$ (CuCl) films thermally treated in air at temperatures T: 1-150 K, 2-200 K, 3-250 K. For comparison, the temperature dependence of the quenching magnitude of the equilibrium conductivity Γ_T (curve 4) and the infrared quenching spectrum of the photoconductivity Γ_{IR} (curve 1', T=150 K) are shown.

Figure 4 shows the infrared quenching spectra of the equilibrium conductivity of the films for three temperatures (curves 1-3). It is convenient to describe the quenching of the dark current (i.e. conductivity) by the relative value $\Gamma = \frac{j_0 - j}{j}$, where j_0 and j are the current densities without and with infrared radiation thermal quenching. As can be seen from the figure, with increasing temperature, the amplitude and half-width of the IQDC spectrum decrease and its red edge shifts significantly towards shorter wavelengths. At T=150 K, the IQDC spectrum, as well as the quenching spectrum of the infrared photoconductivity (curve 1'), reveals a doublet structure with red edges at $\lambda_{r'} = 2.8$ µm. This indicates that at a certain temperature, the equilibrium conductivity in the film is determined by the presence of two recombination centers, one of which has an activation energy of $E_{r'} \approx 0.44$ eV. If we assume, as in the case of single crystals [13], that the $E_{r'}$ level is located close to the edge of the valence band and effectively exchanges carriers with this band, then the "small" TQDC (interval I in Figure 3) and the long-wavelength line of IQDC at low temperatures are associated with the generation or transfer of heat by the infrared radiation of carriers from the r′-center to the valence band. As the temperature increases, the r′-centers become filled and the equilibrium recombination current is captured by deeper centers. These deeper centers now determine the capture time of electrons in the sample, and therefore define the larger quenching intervals of TQDC and the shorter wavelength line of TQDC. From the red edge of this line at T=250 K, we find $\lambda_r = 2\ \mu m$ ($E_r \approx 0.62$ eV). For comparison, Figure 4 shows the temperature dependence of the quenching magnitude of the equilibrium conductivity Γ_T (curve 4). It can also be seen from the figure that infrared quenching was not observed at T=300 K.

To clarify the nature of the observed TQDC and IQDC phenomena, Hall measurements were performed on the studied $CdSe_xS_{1-x}$ films to determine the average mobility μ_H and electron concentration n in the dark (T). The temperature dependence of $\mu_H(T)$ and $n(T)$ is shown in Figure 5, where curves 1-3 are experimental curves corresponding to curves 1-3 in Figure 4, and curves 1'-3' are calculated using $\mu_H = R_H\sigma_d$, where R_H is the Hall coefficient. It is evident that all dependencies $\mu_H(T)$, $n(T)$, $\sigma_d(T)$ are similar at temperatures close to T=300 K. In the range T=100÷150 K, n, μ_H, and therefore σ_d are practically independent of temperature, which seems to correspond to the decrease in the donor and the tunnel mechanism of electrical conductivity in polycrystalline semiconductors.

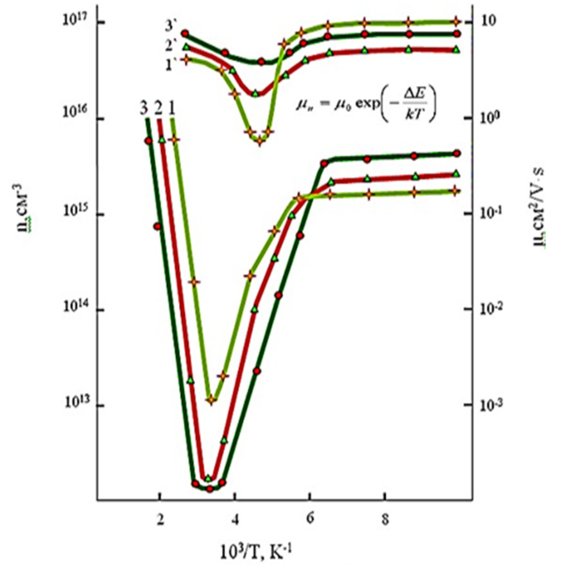

Figure 5. Temperature dependence of the Hall concentration of equilibrium electrons n (1-3) and mobility μ_H (1'-3'). Curves 1-3 and 1'-3' correspond to the description of the sample heating conditions in (Figure 3).

If the Hall mobility of equilibrium electrons μ_H is related to the average height of the drift barriers ΔE_μ

$$\mu_H = \mu_0 \exp\left(-\frac{\Delta E_\mu}{kT}\right),$$

Here, μ_H is the Hall mobility in a homogeneous sample, equal to 200 $sm^2/(V\ s)$. Then, in the regions of curves 1'-3' in the temperature range 150÷300 K, there is a temperature quenching (μ_H) (i.e., we have an anomalous dependence), and at T>300 K, ($d\Delta E_\mu/dT > 0$). Interestingly, for the sample $CdSe_xS_{1-x}$ (CuCl) in the quenching region, the mobility changes with temperature as $\mu \sim T^{-3/2}$, and after quenching, it increases exponentially according to the activation energy $\Delta E_\mu = 0.11$ eV. Furthermore, in all samples, small quenches in the $\mu_H \sim T^{-5/2}$ and $\mu_H \sim T^{-7}$ regions and large quenches in the $\mu_H \sim T^{-5/2}$ and $\mu_H \sim T^{-7}$ temperature ranges correspond to the $CdSe_xS_{1-x}$ (CdCl) and samples, respectively. For the second one, the Hall mobility at temperatures above 300 K first increases according to the laws $\mu_H \sim T^3$ and $\mu_H \sim T^5$, and then exponentially with activation energies of 0.13 and 10 eV. The complex temperature dependence of $\mu_H(T)$ around the temperature quenching naturally reflects the scattering mechanism of electrons at drift barriers. As the temperature increases, the significant decrease in electron concentration leads to the expansion, overlapping, and increase in height of neighboring potential barriers, as well as the emergence of new drift barriers. The sharp difference in temperature dependence of $\mu_H(T)$ in different samples is related to the different crystalline structures of the films, the impurities in them, and the specific defects. The effect of TQDC and IQDC studied cannot be explained using the model of photoconductivity of the same semiconductor containing two or more types of recombination centers [14]. The obtained experimental results also do not fit within the framework of the model in [3], where the negative temperature dependence of the equilibrium carrier concentration is calculated when there is a heterojunction between a low-resistance surface-near region and a high bulk resistance semiconductor. Although the above experimental results clearly indicate the role of volume recombination r-, r'-, s-centers and surface states in the correlation processes, as well as the thermal modulation of drift barriers associated with them, the mechanism of manifestation of these processes in TQDC and IQDC phenomena, at first glance, is not entirely clear within the framework of known models of photoconductivity quenching. Nevertheless, the observed effect can be qualitatively described as follows.

Let's consider a physical model of a bicrystal, corresponding to two adjacent grain boundary regions of a polycrystalline compensated semiconductor with *n*-type conductivity, containing fast (s) and slow (r) recombination volume centers (Figure 6). In equilibrium, due to the upward bending of energy levels near the interface of adjacent crystallites. Under the effective influence of surface acceptor levels, the recombination r-centers in the space charge region, unlike the quasineutral bulk, are partially filled, and the s-centers associated with doubly charged cadmium vacancies V''_{Cd} become vacant and transform into a singly charged state V'_{Cd} (r-center), leading to an increase in the concentration of r-centers at the interface. In the space charge region, the absorption of phonons in TQDC or IQDC quanta can lead to the transition of IQDC electrons from the valence band to empty levels at r-centers. In this case, the generated free hole participates in recombination processes with free electrons of the conduction band either through r- and s-centers or through surface levels, resulting in a decrease in the average concentration of conduction band electrons and dark conductivity.

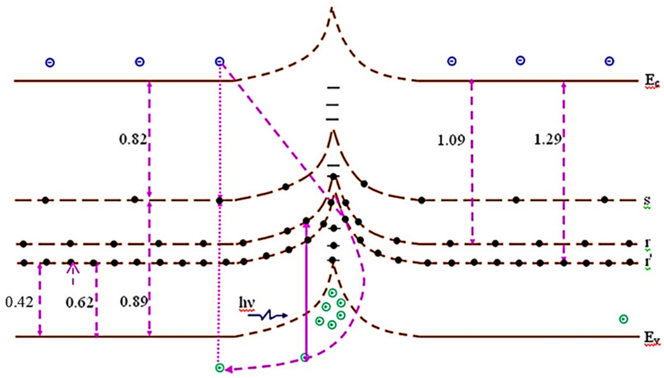

Figure 6. Schematic of a bicrystal model with volume r- and s-recombination centers, showing electron transitions that lead to quenching of dark conductivity with temperature or infrared irradiation.

CONCLUSION

The temperature and infrared quenching of equilibrium conductivity σ_d is observed only in optimally photosensitive samples with r and s recombination centers and effectively working inter-crystallite barriers. They are not observed in freshly evaporated films with a thin fine-grained structure and a thickness of less than 1 micron. It's interesting to note that the quenching of both equilibrium conductivity and photoconductivity occurs within almost identical temperature (150÷300 K) and spectral (1.0÷3.0 μm) ranges. The dependence $\sigma_d(T)$, as well as $\sigma_{ph}(T)$, consists of two parts: 1) a slow decrease with an activation energy $E_{r'}$~$0.14-0.4$ eV (150÷230 K); 2) a sharp decrease with $E_{r'}$~$0.6-1.0$ eV (230÷300 K).

The infrared quenching of equilibrium conductivity is observed at T<300 K and low infrared light intensities $I_{IR} < 10^{-1}$ lx in the input spectral absorption range of 1.0÷3.0 μm. However, with higher intensities $I_{IR} \geq 10^{-1}$ lx, a clear induced photoconductivity is observed.

It's interesting that no significant residual conductivity was found in the temperature quenching of dark conductivity within the samples. This could be attributed to the specific thermal treatment technology used, which might lead to a uniform spatial distribution of inter-crystal point barriers.

It's noteworthy that there was no significant decrease in the influence of TQDC and IQDC throughout the year. However, various external factors significantly impact the movement of charge carriers, leading to the loss of the sample's high photosensitivity. These factors include prolonged high-temperature, laser or ultrasonic treatment in different environments; mechanical deformations with sufficiently large amplitudes $\varepsilon > 10^{-2}$ and a large number of cycles N>500.

It's worth noting that the studied polycrystalline $CdSe_xS_{1-x}$(Cd:Cu:Cl) samples can be used as thermal switches in the temperature range T=150÷300 K and as weak IQ radiation detectors in the $\lambda = 1 \div 3$ μm range at T<300 K.

ORCID

Valijon T. Mirzaev, https://orcid.org/0000-0002-8382-6750; **Bozorboy J. Akhmadaliyev,** https://orcid.org/0000-0003-1930-8649
Iftikhorjon I. Yulchiev, https://orcid.org/0000-0001-9346-0441; **Muminjon M. Madraximov,** https://orcid.org/0000-0001-5435-1242
Tokhirbek I. Rakhmonov, https://orcid.org/0000-0002-6080-6159

REFERENCES

[1] S.N. Moger, and M.G. Mahesha, "Investigation on spectroscopic and electrical properties of p-Si/CdS_xSe_{1-x}(0≤x≤1) heterostructures for photodetector applications," Journal of Alloys and Compounds, **870**, 159479 (2021). https://doi.org/10.1016/j.jallcom.2021.159479

[2] P. Lv, Y. Sun, L. Sui, Z. Ma, K. Yuan, G. Wu, *et al*., "Pressure-Tuned Core/Shell Configuration Transition of Shell Thickness-Dependent CdSe/CdS Nanocrystals," The Journal of Physical Chemistry Letters, **11**(3), 920-926 (2020). https://pubs.acs.org/doi/10.1021/acs.jpclett.9b03650

[3] M. Ajibzhanov, M.A. Karimov, M.S. Saudov, and N.K. Yuldashev, "An anomalous temperature dependence and infrared extinction of equilibrium conductivity in polycrystalline CdSe films," Fizika i tekhnika poluprovodnikov, **30**(9), 1578–1584 (1996).

[4] M.A. Karimov, and N.H. Yuldashev, "Obliquely deposited CdTe: In films with anomalous photovoltaic properties," Bulletin of the Russian Academy of Sciences: Physics, **71**, 1151-1153 (2007). https://doi.org/10.3103/S1062873807080291

[5] N.K. Yuldashev, D.T. Mamadieva, V.T. Mirzaev, and D.S. Xidirov, "Effect of Heat Treatment Conditions on Photo sensitivity of $CdSe_xS_{1-x}$ Polycrystalline Films," Journal of Applied Mathematics and Physics, **10**(10), 3208-3217 (2022). https://doi.org/10.4236/jamp.2022.1010213

[6] Polvonov, B. Z., & Yuldashev, N. K. (2016). Spectra of low-temperature photoluminescence in thin polycrystalline CdTe films. Semiconductors, 50, 1001-1004. https://doi.org/10.1134/S1063782616080194

[7] G. Lucovsky, "On the photoionization of deep impurity centers in semiconductors," Solid state communications, **88**(11-12), 879-882 (1993). https://doi.org/10.1016/0038-1098(93)90261-K

[8] A.S. Hassanien, and A.A. Akl, "Effect of Se addition on optical and electrical properties of chalcogenide CdSSe thin films," Superlattices and Microstructures, **89**, 153-169 (2016). https://doi.org/10.1016/j.spmi.2015.10.044

[9] J. Sharma, G.S.S. Saini, N. Goyal, and S.K. Tripathi, "Thermally induced changes on the electrical and optical properties of nanocrystalline CdSe thin films," Journal of optoelectronics and advanced materials, **9**(10), 3194 (2007). https://www.researchgate.net/publication/216691417

[10] P.K.C. Pillai, N. Shroff, N.N. Kumar, and A.K. Tripathi, "Photoconductivity and dark-conductivity studies of $CdS_{1-x}Se_x$(Cu) sintered layers," Physical Review B, **32**(12), 8228 (1985). https://doi.org/10.1103/PhysRevB.32.8228
[11] M. Ayibzhanov, O. Mamatov, V. Mirzaev, and B. Tuychibaev, "Luminescence spectrum of cadmium chalcogenide photovoltaic film structures and their power enhancement," E3S Web of Conferences, **583**, 04003 (2024). https://doi.org/10.1051/e3sconf/202458304003
[12] B. Akhmadaliyev, T. Rakhmonov, K. Sulaimonov, and O. Nurmatov, "Photocunductivity spectra of thin solid solution films $CdSe_xS_{1-x}$," E3S Web of Conferences, **583**, 04002 (2024). https://doi.org/10.1051/e3sconf/202458304002
[13] Y.V. Trofimov, L.N. Survilo, E.F. Ostretsov, and M.S. Tivanov, "Physicochemical features of dielectrical nano-barrier layers in CdSexS1-x films formed by screen printing method," Lithuanian Journal of Physics, **52**(3), 219–223 (2012). https://doi.org/10.3952/physics.v52i3.2473
[14] A.S. Abdinov, M.A. Jafarov, N.M. Mechtiyev, E.F. Nasirov, and H.M. Mamedov, "Photodetectors of IR radiation on the basis of $CdS_{1-x}Se_x$ films deposited from solution," in: *16th International Conference on Photoelectronics and Night Vision Devices*, vol. 4340, pp. 107-111 (2000). SPIE. https://doi.org/10.1117/12.407716
[15] M.A. Karimov, and N.H. Yuldashev, "Obliquely deposited CdTe:In films with anomalous photovoltaic properties," Bull. Russ. Acad. Sci. Phys. **71**, 1151–1153 (2007). https://doi.org/10.3103/S1062873807080291
[16] Z.X. Mirzajonov, K.A. Sulaymonov, T.I. Rakhmonov, F.T. Yusupov, D.Sh. Khidirov, and J.S. Rakhimjonov, "Advancements in Zinc Oxide (ZnO) thin films for photonic and optoelectronic applications: a focus on doping and annealing processes," E3S Web of Conferences, **549**, 03013 (2024). https://doi.org/10.1051/e3sconf/202454903013
[17] B.Z. Akhmadaliev, N.K. Yuldashev, and I.I. Yulchiev, Surface-Radiative Modes and Longitudinal Excitons in the Spectra of Exciton–Polariton Luminescence. Opt. Spectrosc. **125**, 343–352 (2018). https://doi.org/10.1134/S0030400X18090023
[18] F.T. Yusupov, T.I. Rakhmonov, M.F. Akhmadjonov, M.M. Madrahimov, and S.S. Abdullayev, "Enhancing ZnO/Si Heterojunction Solar Cells: A Combined Experimental and Simulation Approach," East European Journal of Physics, (3), 425-434. https://doi.org/10.26565/2312-4334-2024-3-51

ТЕМПЕРАТУРА ТА ІНФРАЧЕРВОНЕ ГАСІННЯ РІВНОВАЖНОЇ ПРОВІДНОСТІ В ПЛІВЦІ $CdSe_xS_{1-x}$

Валіджон Т. Мірзаєв, Бозорбой Дж. Ахмадалієв, Іфтіхорджон І. Юлчієв, Мумінджон М. Мадраксимов, Тохірбек І. Рахмонов
Ферганський державний технічний університет, Фергана, Узбекистан

Розроблено метод отримання *CdSe, $CdSe_xS_{1-x}$* плівок з високою світлочутливістю. Цей метод передбачає термічну обробку свіжоприготованих плівок у вакуумі та на повітрі в спеціально підготовленій квазігерметичній камері в присутності $CdCl_2$ або $CuCl_2$, що забезпечує рівномірну дифузію сенсибілізуючих речовин. Експерименти показали, що *CdSe, $CdSe_xS_{1-x}$* плівки зі стабільними та відтворюваними електрофізичними властивостями отримують шляхом нагрівання за таких температур: на повітрі в присутності $CdCl_2$ – 470°C; у присутності $CuCl_2$ – 300°C; у вакуумі – 480°C. Температурне та інфрачервоне гасіння рівноважної провідності спостерігається лише в оптимально світлочутливих. зразки як з швидкими (r), так і з повільними (s) центрами рекомбінації та ефективно працюють міжкристалічні бар'єри. Однак різні зовнішні впливи істотно впливають на рух носія, що призводить до втрати високої світлочутливості зразка. Інфрачервоне гасіння рівноважної провідності спостерігається на $T < 300\ K$ і низькій інтенсивності інфрачервоного світла $I_{IR} < 10^{-1} lx$ у вхідному діапазоні спектрального поглинання 1.0 ÷ 3.0 μm, а виражена фотопровідність з чітко визначеним входом спостерігається на $I_{IR} \geq 10^{-1} lx$.

Ключові слова: *фоточутливість; CdSe, $CdSe_xS_{1-x}$; квазізакрита камера; термообробка; температурне та інфрачервоне гасіння; поле просторового заряду; дрейфові бар'єри; розмір зерен*